Consideration of cold metal transfer welding of AA5754 to galvanized steel from mechanical and microstructural aspects

Nilay Çömez[a,✉], Hülya Durmuş[a]

[a] Manisa Celal Bayar University, Engineering Faculty, Department of Metallurgical and Materials Engineering, Manisa, Turkey
[✉]Corresponding author: nilay.comez@cbu.edu.tr

ABSTRACT: In this study, overlap welding of AA5754 and galvanized steel sheets was carried out by cold metal transfer (CMT) method using ER4043 (AlSi$_5$) filler wire. The effect of heat input on the formation of intermetallic compound (IMC) layer between steel and aluminum was investigated. Mechanical properties of the joints were determined by tensile and hardness tests and also applying nano indentation test to intermetallic layer. Chemical compositions of IMC were analyzed by EDX and the formation of Al$_{7.2}$Fe$_{1.8}$Si and Fe$_2$Al$_5$ phases was detected. Formation of Fe$_2$Al$_5$ phase was found detrimental for reliability of joint, although it's superior mechanical strength.

KEYWORDS: Aluminum; Intermetallic; Steel; Welding

RESUMEN: *Consideración sobre la soldadura de transferencia de metal frio de AA5754 al acero galvanizado a partir de aspectos mecánicos y microestructurales*. En este estudio, la soldadura por solapamiento de AA5754 y chapas de acero galvanizado se llevó a cabo mediante el método de transferencia de metal en frío (CMT) utilizando un hilo de relleno ER4043 (AlSi$_5$). Se investigó el efecto del aporte de calor sobre la formación de la capa de compuesto intermetálico (IMC) entre el acero y el aluminio. Las propiedades mecánicas de las juntas se determinaron mediante ensayos de tracción y dureza y también aplicando la prueba de nano indentación a la capa intermetálica. Las composiciones químicas de IMC se analizaron mediante EDX y se detectó la formación de fases Al$_{7.2}$Fe$_{1.8}$Si y Fe$_2$Al$_5$. La formación de la fase Fe$_2$Al$_5$ fue perjudicial para la fiabilidad de la articulación, aunque su resistencia mecánica es superior.

PALABRAS CLAVE: Acero; Aluminio; Intermetálico; Soldadura

ORCID ID: Nilay Çömez (https://orcid.org/0000-0002-6432-6582); Hülya Durmuş (https://orcid.org/0000-0002-7270-562X)

1. INTRODUCTION

The necessity for joints between dissimilar materials often arises in functionally complex industrial applications, economic and environmental concerns (Torkamany *et al.*, 2010; Guo *et al.*, 2014; Liu *et al.*, 2015). For instance, the combination of steel with aluminum provides fuel-efficiency by reducing the weight of construction (Miller *et al.*, 2000; Torkamany *et al.*, 2010; Ahsan *et al.*, 2016). One of the major challenges in transportation vehicle manufacturing is the joining of aluminum and

steel by conventional fusion welding methods due to the large difference between their physical and chemical properties (Cao *et al.*, 2014a ; Guo *et al.*, 2014; Squires *et al.*, 2015).

Al-Fe phase diagram reveals that the solid solubility of iron in aluminum is quite low (Torkamany *et al.*, 2010; Su *et al.*, 2014). Hence, the formation of brittle intermetallic phases such as Fe_3Al, $FeAl$, $FeAl_2$, Fe_2Al_3, Fe_2Al_5 and $FeAl_3$ are promoted especially at high temperature (Potesser *et al.*, 2006; Torkamany *et al.*, 2010; Cao *et al.*, 2013; Zhou and Lin, 2014; Liu *et al.*, 2015). Fe-Al intermetallic phases are required for an effective joint between aluminum and steel, nevertheless thickness of this IMC layer should be kept below 10 µm to supply technical demands (Jácome *et al.*, 2009; Cao *et al.*, 2014a). In order to control the thickness of Fe-Al intermetallic layer, weld heat input should be kept at a low rate.

Recently developed cold metal transfer (CMT) welding which is characterized with low heat input and spatter free weld, is recommended for joining dissimilar materials (Yang *et al.*, 2013; Ahsan *et al.*, 2016). In CMT welding, filler wire is withdrawn after short-circuiting and the metal transfer takes place by the detachment of the molten droplet with the aid of the wire movement (Yang *et al.*, 2013; Zhang *et al.*, 2013; Ahsan *et al.*, 2016).

CMT welding of AA6061 to galvanized steel was studied by numerous researchers (Agudo *et al.*, 2007; Cao *et al.*, 2013; Yang *et al.*, 2013; Zhang *et al.*, 2013; Cao *et al.*, 2014b). However, there is limited number of studies about CMT welding of AA5754 to steel in literature. AA5754 sheets are employed in inner panels of automobiles (Davies, 2003; Halim *et al.*, 2007). As is known, numerous steel grades are the major materials of vehicle structures. These steels are mostly coated with zinc to provide galvanic protection (Ahsan *et al.*, 2016). Zhou and Lin (2014) reported that zinc coating provides wettability of aluminum on the steel surface and also some heat can be removed from the system with the help of zinc vaporization.

AA5754 to steel joints were studied by several researchers. Figner *et al.* (2009) examined the friction stir spot welding of aluminum AA5754 and galvanized steel HX 340LAD. Yang *et al.* (2015) studied lap joining of AA5754 to DP 980 steel by diode laser welding and investigated the correlation between interfacial microstructure and mechanical properties. They obtained a hard and a brittle $Fe_2(Al,Si)_5$ (η phase) with micro cracks between steel and aluminum at high laser power. Watanabe *et al.* (2006) joined 2 mm thick SS400 carbon steel and AA5083 with friction stir welding. According to their study IMCs was found to be detrimental for joint strength. They also observed large pores at the Al/Fe interface.

Present study is aimed to research the weldability of AA5754 to galvanized steel which may provide benefit for automotive applications. For this purpose, effect of heat input on correlation between intermetallic formation and mechanical properties of joints was investigated. The originality of this study is the interpretation of tensile strength according to hardness and elastic modulus of intermetallic phases which were determined by nano indentation test.

2. MATERIALS AND METHODS

2 mm thick AA5754 (Table 1) and galvanized steel sheets (EN 10143 – DX 51D+Z) (Table 2) were joined with CMT overlap welding, using ER4043 filler material (Table 3) having a diameter of 1.2 mm. In order to remove the oxide layer, welding groove of aluminum sheets were grinded and wiped with acetone. Weld pool was isolated by argon gas (15 l·min⁻¹) during the welding process. Welding parameters are given in Table 4. Torch angle and distance between the torch and the work piece were adjusted to 90° and 12 mm respectively.

2.1. Microstructural investigations: OM and SEM-EDX

Cross-sections of welded specimens were grinded and polished. Keller and Nital reagents were used for the etching of aluminum weld metal and galvanized steel, respectively. AA5754 base metal was etched with a solution consists of 20 g NaOH

TABLE 1. Typical chemical composition of AA5754 (wt.%)

Mg	Mn	Fe	Si	Al
2.6-3.2	0.5	0.4	0.4	Rest

TABLE 2. Typical chemical composition of steel (wt.%)

C	Mn	P	S	Si	Ti	Fe
0.051	0.216	0.018	0.013	0.014	0.001	Rest

TABLE 3. Typical chemical composition of ER4043 (wt.%)

Si	Mn	Fe	Zn	Cu	Ti	Al
5	<0.01	<0.3	<0.01	<0.01	<0.01	Rest

TABLE 4. Welding parameters

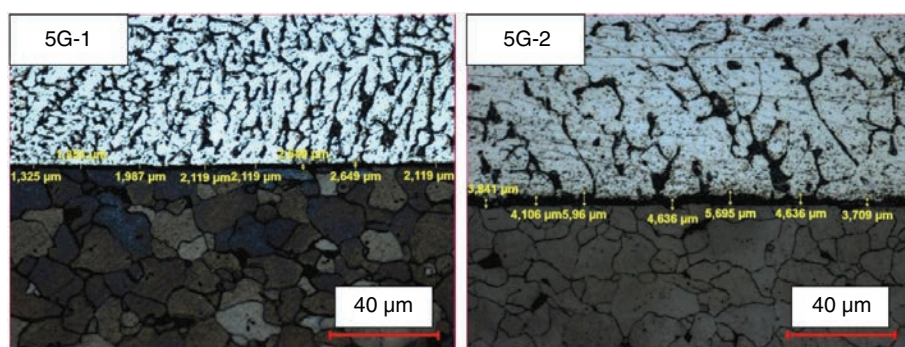| Sample	5G-1	5G-2
Welding speed (m·min⁻¹)	1	0.5
Current (A)	82±1	
Voltage (V)	11.3±0.1	
Wire feed rate (m·min⁻¹)	4.8±0.1	
Heat input (J·mm⁻¹)	49.86	100.4

FIGURE 1.   IMC layer thicknesses of CMT welded samples.

and 100 ml distilled water. Nikon LV150 optical microscope and Clemex software were used for microstructural investigation of the weld zone and measuring the thickness of the intermetallic layers. Chemical composition of intermetallic phases was determined by SEM-EDX. XRD analysis was applied to Al/steel interface of 5G-2 which separated during the tensile test.

2.2. Tensile test

Mechanical strength of the welded specimens was determined by Shimadzu Autograph tensile testing device with the rate of 1 mm·min^{-1} at room temperature using extensometer. Tensile tests were conducted according to DIN EN 895 standard. Three specimens of each welding parameters were tested and the average results of tensile strength were calculated.

2.3. Micro hardness test and nano indentation test

Micro hardness test was carried out in order to detect the heat affected zone. Vickers micro hardness values were measured in the order of aluminum-weld seam-steel using Future-Tech FM700, under 100 gf (gram-force) load applied for 10 seconds.

Berkovich indenter was utilized for the nano indentation test, which was carried out under 5 mN load in an attempt to determine the elastic modulus and the hardness of Al/Fe IMCs.

3. RESULTS AND DISCUSSION

3.1. Microstructural investigations

The cross-sectional microstructures of CMT welded AA5754 and galvanized steel are presented in Fig. 1. The grain size of steel base metal did not change by the heat input, while the aluminum weld metal grains became coarser with the increasing weld heat. Steel substrate and aluminum base metal generated a temperature gradient which caused the formation of columnar grain
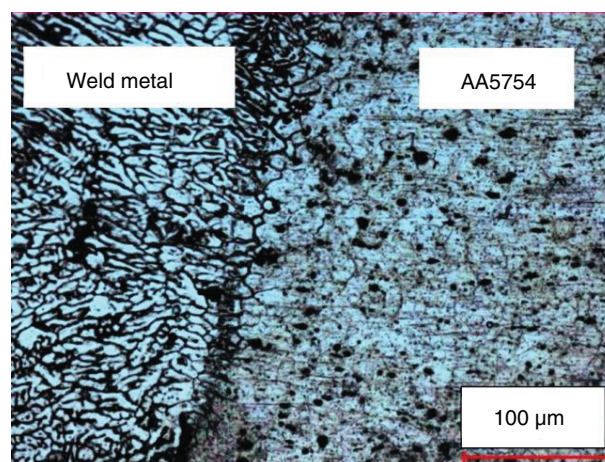

FIGURE 2.   AA5754/weld metal interface of 5G-1.

growth in the weld metal adjacent to steel and AA5754 (Fig. 1 and Fig. 2). Increasing weld heat input promoted the growth of Al/Fe IMC layer. Mean intermetallic thickness values of 5G-1 and 5G-2 were calculated as 2.103 µm and 4.655 µm respectively.

Torkamany *et al.* (2010) joined 0.8 mm thick low carbon steel (st14) and 2 mm thick AA5754 with Nd:YAG laser welding. They reported the formation of cracks, pores and cavitation in intermetallic layer between Al/Fe interfaces. They also mentioned that with the increasing laser peak power and the heat input, the percentage of IMC raised in weld metal. In present study, cracks or pores were observed in neither microstructure nor SEM investigations of IMC layers.

As is seen from Fig. 3, the intermetallic compound grew towards aluminum weld metal. This phenomenon can be explained with diffusion mechanisms and characteristics of Al and Fe elements. Shao *et al.* (2015) reported that iron atoms could diffuse more easily in liquid aluminum weld metal by virtue of the higher diffusion coefficient of iron in liquid aluminum in comparison with the diffusion coefficient of aluminum in solid iron.

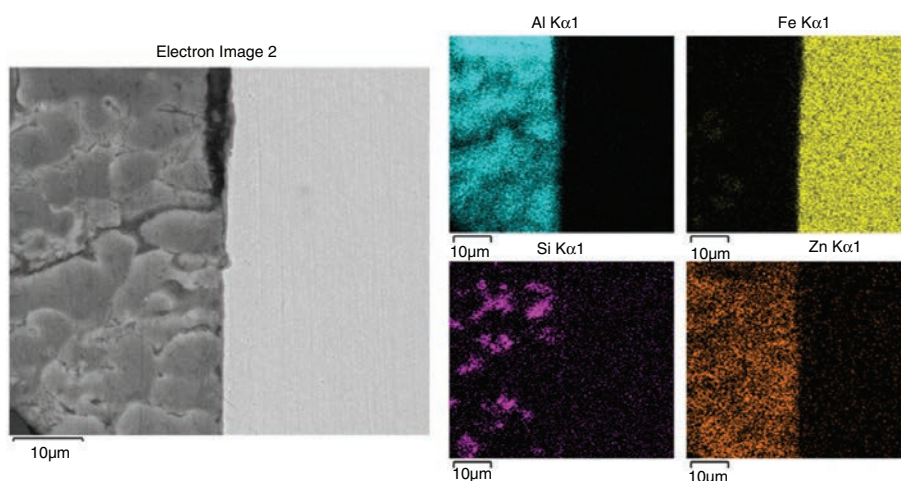FIGURE 3.   Growth of intermetallic layer towards aluminum .

FIGURE 4.   Elemental mapping from the Zn rich zone of 5G-1 weld metal.

In Fig. 4 SEM-EDX analysis of the weld toe of sample 5G-1 is given. It was observed that the IMC layer disappeared and Al weld metal exhibited cellular structure. Elemental mapping revealed that this region contains a large amount of Zn in Al weld metal (Fig. 4). When the molten aluminum droplet detaches from the wire, it replaces with zinc (melting point~420 °C) in liquid state. Although the density of liquid zinc (6.57 g·cm^{-3}) is almost 3 times greater than that of aluminum, in present study it was observed that with the aid of both weld arc forces and mass of molten filler wire, liquid zinc was swept towards the toe of weld metal.

It was thought that, this phenomenon was also supported by the tendency of aluminum to form Al/Fe IMCs with iron. Zhou and Lin (2014) stated that the replacement of aluminum and zinc occurs due to the higher tendency and reactivity of aluminum to iron than that of zinc to iron. They have proved their thesis with EDS analyses of interface and end point of weldment. They did not encounter any Zn trace at the interface of aluminum and steel. Besides, they observed zinc liquid film accumulated at the weld toe.

Another remarkable finding is the accumulation of zinc at the end of aluminum weld metal instead

of steel base metal (Fig. 4). Zn has a higher affinity to Al than to Fe; hereby Al-Zn phases are formed at the weld toe (Agudo *et al.*, 2007).

3.2. Chemical analysis of intermetallic phases

EDX analyses of intermetallic layers were carried out as shown in Fig. 5. EDX results are presented in Table 5. Silicon content was detected to be higher in the intermetallic layer of 5G-1 than that of 5G-2. Silicon avoids the growth of Al/Fe phases by occupying the vacancies of the Al/Fe intermetallic compounds and forms $Fe_xAl_ySi_z$ phases which possess a slower growing rate than Fe_xAl_y phases (Eggeler *et al.*, 1986; Jácome *et al.*, 2009). As a result, intermetallic compound layer of 5G-2 exhibited finger-like growth towards aluminum while the intermetallic layer of 5G-1 grew smoothly due to the suppression of Si atoms (Fig. 5).

Chemical compositions of some Al/Fe and Al/Fe/Si IMCs are listed in Table 6 based on the literature findings. It was noticed that the chemical composition of 5G-1 was found to be similar to $Al_{7.2}Fe_{1.8}Si$ phase as mentioned in (Song *et al.,* 2009; Yang *et al.*, 2015).

According to Al-Fe binary phase diagram, Fe_2Al_5 compound contains 53-57 wt.% aluminum (Kattner and Burton, 1992). Formation of brittle Fe_2Al_5 intermetallic phase was approved by EDX analysis of 5G-2 which can also be supported by the findings of (Maitra and Gupta, 2002; Agudo *et al.*, 2007; Cao *et al.*, 2014b) (Table 6).

Although Fe_xAl_y phases are required for an effectual joint between aluminum and steel, excessive formation of these phases leads to the tendency of crack initiation in intermetallic layer under tensile stress (Agudo *et al.*, 2007; Su *et al.*, 2014). As is known, the growth of brittle Al/Fe IMCs can be replaced with less detrimental Al/Fe/Si phases by Si addition (Song *et al.*, 2009). Apart from the control of intermetallic layer thickness, mechanical properties of dissimilar Al-steel joints can also be adjusted with the aid of Si based filler wires. Although $Al_{7.2}Fe_{1.8}Si$ phase hinders the growth of Fe_xAl_y phases (Song *et al.*, 2009), increasing the heat input led to the formation of brittle Fe_2Al_5 compound in present study.

The result of XRD analysis taken from Al/steel interface of 5G-2 shows the peaks of Al, Fe and Zn elements as expected; in addition it indicates the probable existence of AlZn and Fe_2Al_5 intermetallics (Fig. 6).

3.3. Tensile test

Hybrid structures such as dissimilar welding of aluminum and steel keep various phases with different physical and chemical properties together. For instance, Al/Fe IMCs exhibit superior mechanical properties in comparison to metallic materials. As a result, their respond to mechanical forces will not be similar to aluminum and steel. Therefore mechanical tests should be carried out to understand the fracture mechanism and ultimate tensile strength of hybrid joints in order to build safe constructions.

Stress-strain curves of CMT welded AA5754-galvanized steel joints are given in Fig. 7. CMT welded AA5754-galvanized steel samples exhibited different deformation and fracture characteristics.
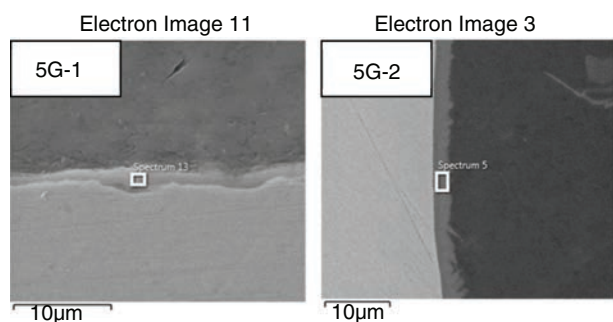

FIGURE 5. SEM-EDX analyses of intermetallic layer.

TABLE 5. SEM-EDX results of intermetallic compound layers

Element	5G-1		5G-2	
	wt.%	at.%	wt.%	at.%
Al	59.88	72.06	56.24	69.49
Si	8.40	9.71	4.35	5.16
Fe	29.17	16.96	38.18	22.79
Zn	2.55	1.27	1.23	2.56
Total	100.00	100.00	100.00	100.00

TABLE 6. Al/Fe IMC compositions from literature

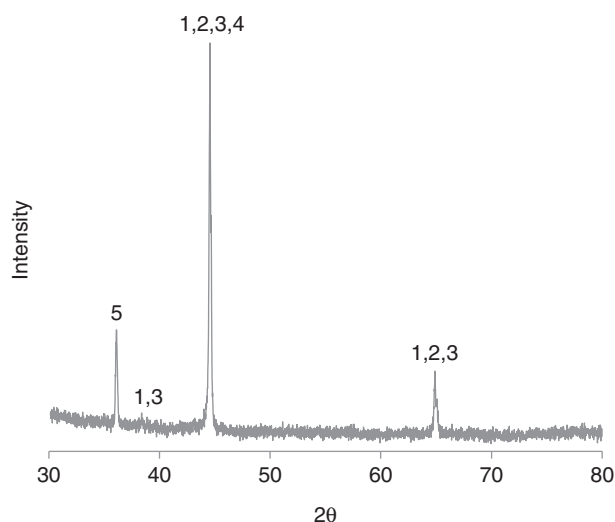| Phase	Fe	Al	Si	Reference
Fe_2Al_5 (at.%)	28.1	67.24	4.66	(Maitra and Gupta, 2002)
	27	68	-	(Agudo *et al.,* 2007)
	24.91	69.43	5.66	(Cao *et al.,* 2014a)
$Fe_2(Al,Si)_5$ (at.%)	29.4±0.1	66.3±1.6	4.3±0.9	(Yang *et al.,* 2015)
$Al_{7.2}Fe_{1.8}Si$ (at.%)	18.4±1.9	73.5±1.2	8.1±1.7	(Yang *et al.,* 2015)
$Al_{7.2}Fe_{1.8}Si$ (wt.%)	21.66	63.54	9.84	(Song *et al.,* 2009)

FIGURE 6.   XRD analysis from Al/steel interface of 5G-2.
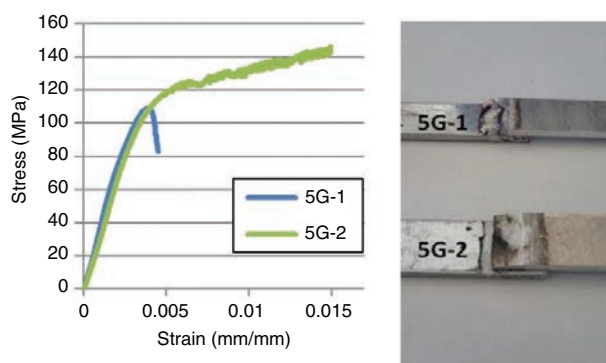(1: Al, 2: Fe, 3: AlZn, 4: Fe_2Al_5, 5: Zn).

FIGURE 7.   Stress-strain curves and fracture locations
of AA5754-galvanized steel joints.

AA5754 aluminum alloy shows discontinuous deformation at room temperature which is called Portevin–Le Chatelier (PLC) effect. This effect is categorized according to serration types in the stress–strain curve (Halim *et al.*, 2007). In this study, sample 5G-2 presents Type-B serrations which show hopping propagation (Halim *et al.*, 2007) as it can be seen in Fig. 7. Although the PLC effect was observed clearly in plastic deformation zone of the sample 5G-2 (AA5754 base metal, Fig. 7), the fracture occurred at the Al/steel interface instead of the AA5754 base metal. It was thought that cracks initiated at the brittle Fe_2Al_5 intermetallic layer beyond the threshold load value and propagated rapidly causing an instantaneous rupture of the sample 5G-2. Similarly, the sample 5G-1 also fractured suddenly at the weld seam without plastic deformation (Fig. 7).

Figure 8 presents the fracture surface of 5G-1 which includes numerous micro-scale pores in weld seam. Oxygen and zinc rich zone was observed from the elemental mapping analysis right above the Al/steel interface where the aluminum content decreases.

Su *et al.* (2014) joined AA5052 and galvanized mild steel sheets by alternate-current double pulse gas metal arc welding in lapping configuration with Al–5Si filler wire and obtained a 134 MPa ultimate tensile strength. Song *et al.* (2009) focused on the effect of Si on the formation of Al/Fe intermetallic compounds which takes place in TIG welding of 5A06 aluminum alloy and AISI 321 stainless steel using 1100 pure Al, $AlSi_5$ and $AlSi_{12}$ filler metals. They found that intermetallic layer having 5 wt.% of Si additions showed the optimum mechanical properties with the tensile strength of 125.2 MPa. The tensile strength values of 5G-1 and 5G-2 welded with $AlSi_5$ filler wire were found as 105.29 MPa and 146.3 MPa, respectively. The higher joint strength of the sample 5G-2 is attributed to the formation of Fe_2Al_5 phase which has superior mechanical properties. However, Fe_2Al_5 induced the brittle fracture of intermetallic layer.

3.4. Micro hardness test

Hardness distribution of Al/steel joints was almost homogenous as in Fig. 9. Heat affected zone (HAZ) was not observed both at the AA5754 and steel base metals due to the low heat input characteristics of CMT welding. Microstructural investigations also revealed that grain coarsening which is responsible for the hardness drop did not occur in base metals. Magda *et al.* (2013) reported that CMT did not lead to any changes in the HAZ of the base material. In the present study, a significant change in hardness was not observed, while increasing the heat input caused the grain coarsening of weld metal.

3.5. Nano indentation test

Nano indentation test was applied to intermetallic layers from the cross section of weld metal. Load-displacement (P-h) curves of $Al_{7.2}Fe_{1.8}Si$ and Fe_2Al_5 phases are given in Fig. 10. The effect of silicon content on mechanical properties can be seen clearly from Table 7. $Al_{7.2}Fe_{1.8}Si$ which contains more Si has lower hardness and elastic modulus than that of Fe_2Al_5 with less Si content.

Although the increasing hardness and elastic modulus enhanced the tensile strength of dissimilar AA5754/steel joint, a fracture located at the brittle Fe_2Al_5 intermetallic layer due to the deterioration of plastic strain properties.

4. CONCLUSIONS

AA5754 aluminum alloy and galvanized steel was joined successfully by CMT welding using $AlSi_5$ filler wire. The effect of heat input on the formation
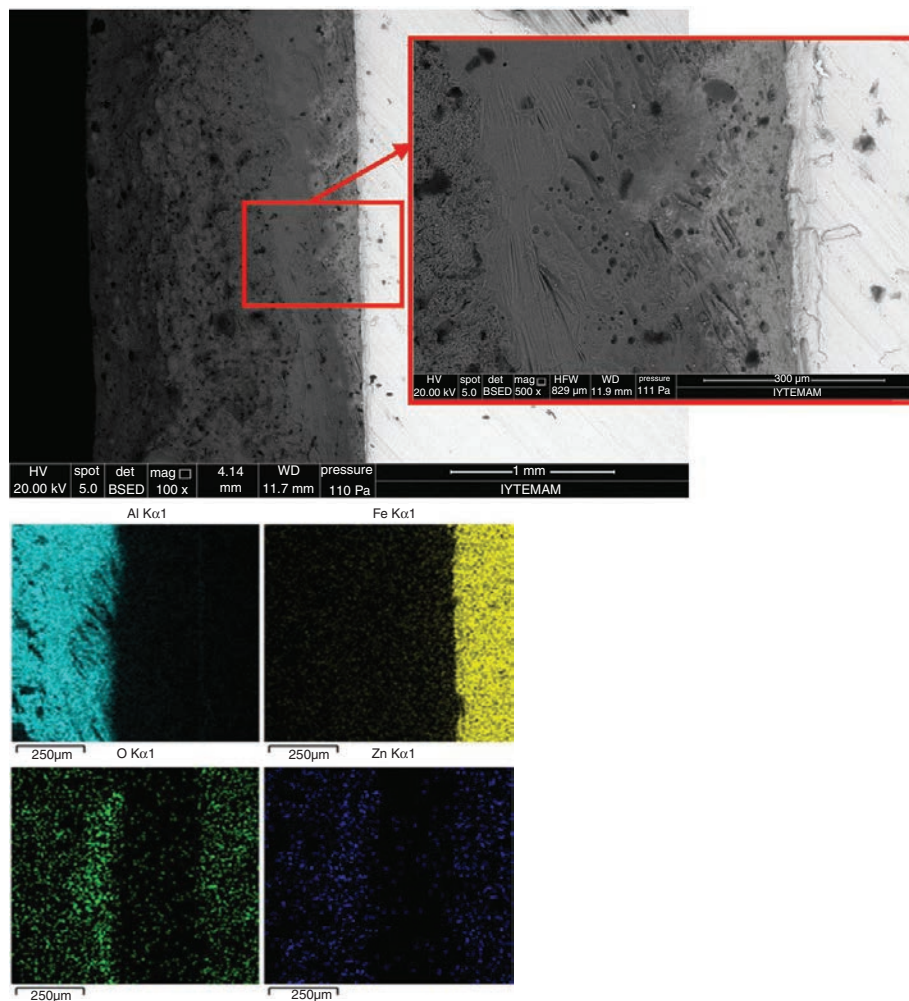
FIGURE 8.   SEM-EDX mapping analysis of fracture surface of the sample 5G-1.
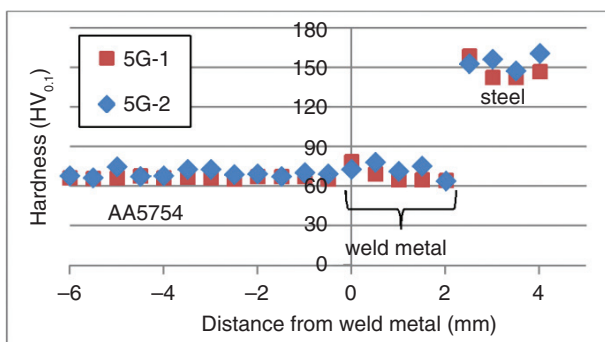

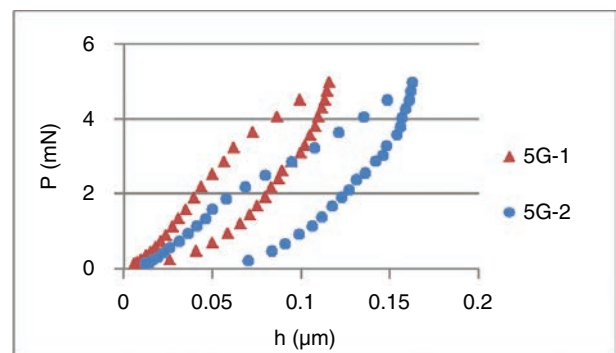FIGURE 9.   Hardness survey of welded samples.

FIGURE 10.   P-h curves of intermetallic phases.

of intermetallic layer and mechanical properties was investigated. The findings can be summarized as follows:

- Both microstructural investigations and micro hardness measurements revealed that CMT welding restrained the HAZ in aluminum and steel base metals. However, increasing the weld heat caused the grain coarsening of weld metal.

- $Al_{7.2}Fe_{1.8}Si$ phase was observed at 49.86 $J \cdot mm^{-1}$ heat input. Increasing heat input promoted the growth of intermetallic layer and also led to the

TABLE 7. Hardness and elastic modulus of intermetallic phases

Sample (Phase)	5G-1 ($Al_{7.2}Fe_{1.8}Si$)	5G-2 (Fe_2Al_5)
Hardness (GPa/HV)	6.49 / 728.72	12.53 / 1277.45
Elastic Modulus (GPa)	303.55	529.98

development of brittle Fe_2Al_5 phase which has superior hardness, elastic modulus and tensile strength of joint in comparison with $Al_{7.2}Fe_{1.8}Si$.

- Although the Fe_2Al_5 phase enhanced the tensile strength due to its brittle characteristic, the fracture occurred at this intermetallic layer. The sample which involves $Al_{7.2}Fe_{1.8}Si$ phase fractured from the weld seam due to the excessive pore formation in the weld metal.

ACKNOWLEDGMENTS

REFERENCES

Agudo, L., Eyidi, D., Schmaranzer, C.H., Arenholz, E., Jank, N., Bruckner, J., Pyzalla, A.R. (2007). Intermetallic Fe_xAl_y-phases in a steel/Al-alloy fusion weld. *J. Mater. Sci.* 42 (12), 4205–4214. https://doi.org/10.1007/s10853-006-0644-0.

Ahsan, M.R.U., Kim, Y.R., Kim, C.H., Kim, J.W., Ashiri, R., Park, Y.D. (2016). Porosity formation mechanisms in cold metal transfer (CMT) gas metal arc welding (GMAW) of zinc coated steels. *Sci. Technol. Weld. Joi.* 21 (3), 209–215. https://doi.org/10.1179/1362171815Y.0000000084.

Cao, R., Yu, G., Chen, J.H., Wang, P.C. (2013). Cold metal transfer joining aluminum alloys-to-galvanized mild steel. *J. Mater. Process. Tech.* 213 (10), 1753–1763. https://doi.org/10.1016/j.jmatprotec.2013.04.004.

Cao, R., Sun, J.H., Chen, J.H., Wang, P.C. (2014a). Weldability of CMT Joining of AA6061-T6 to Boron Steels with Various Coatings. *Weld. J.* 93, 193–204. http://files.aws.org/wj/supplement/WJ_2014_06_s193.pdf.

Cao, R., Huang, Q., Chen, J.H., Wang, P.C. (2014b). Cold metal transfer spot plug welding of AA6061-T6-to-galvanized steel for automotive applications. *J. Alloy. Compd.* 585, 622–632. https://doi.org/10.1016/j.jallcom.2013.09.197.

Davies, G. (2003). *Materials for Automobile Bodies*. Elsevier, Oxford, England.

Eggeler, G., Auer, W., Kaesche, H. (1986). On the influence of silicon on the growth of the alloy layer during hot dip aluminizing. *J. Mater. Sci.* 21 (9), 3348–3350. https://doi.org/10.1007/BF00553379.

Figner, G., Vallant, R., Weinberger, T., Enzinger, N., Schröttner, H., Pašič, H. (2009). Friction Stir Spot Welds between Aluminium and Steel Automotive Sheets: Influence of Welding Parameters on Mechanical Properties and Microstructure. *Weld. World.* 53 (1–2), 13–23. https://doi.org/10.1007/BF03266697.

Guo, J.F., Chen, H.C., Sun, C.N., Bi, G., Sun, Z., Wei, J. (2014). Friction stir welding of dissimilar materials between AA6061 and AA7075 Al alloys effects of process parameters. *Mater. Design* 56, 185–192. https://doi.org/10.1016/j.matdes.2013.10.082.

Halim, H., Wilkinson, D.S., Niewczas, M. (2007). The Portevin–Le Chatelier (PLC) effect and shear band formation in an AA5754 alloy. *Acta Mater.* 55 (12), 4151–4160. https://doi.org/10.1016/j.actamat.2007.03.007.

Jácome, L.A., Weber, S., Leitner, A., Arenholz, E., Bruckner, J., Hackl, H., Pyzalla, A.R. (2009). Influence of Filler Composition on the Microstructure and Mechanical Properties of Steel-Aluminum Joints Produced by Metal Arc Joining. *Adv. Eng. Mater.* 11 (5), 350–358. https://doi.org/10.1002/adem.200800319.

Kattner, U.R., Burton, B.P. (1992). *ASM Handbook Volume 3: Alloy Phase Diagrams*. ASM International, Materials Park, OH, USA.

Liu, J., Jiang, S., Shi, Y., Kuang, Y., Huang, G., Zhang, H. (2015). Laser fusion–brazing of aluminum alloy to galvanized steel with pure Al filler powder. *Opt. Laser. Technol.* 66, 1–8. https://doi.org/10.1016/j.optlastec.2014.08.004.

Magda, A., Popescu, M., Codrean, C., Mocuta, E.G. (2013). Possibilities of joining galvanized sheet steel using the CMT method (cold metal transfer). *Weld. Int.* 27 (9), 665–667. https://doi.org/10.1080/09507116.2011.606137.

Maitra, T., Gupta, S. (2002). Intermetallic compound formation in Fe-Al-Si ternary system: Part II. *Mater. Charact.* 49 (4), 293–311. https://doi.org/10.1016/S1044-5803(03)00005-6.

Miller, W.S., Zhuang, L., Bottema, J., Wittebrood, A.J., De Smet, P., Haszler, A., Vieregge, A. (2000). Recent development in aluminium alloys for the automotive industry. *Mat. Sci. Eng. A-Struct.* 280 (1), 37–49. https://doi.org/10.1016/S0921-5093(99)00653-X.

Potesser, M., Schoeberl, T., Antrekowitsch, H., Bruckner, J. (2006). The Characterization of the Intermetallic Fe-Al Layer of Steel-Aluminum Weldings. *EPD Congress*, San Antonio, Texas, USA. pp. 167–176.

Shao, L., Shi, Y., Huang, J.K., Wu, S.J. (2015). Effect of joining parameters on microstructure of dissimilar metal joints between aluminum and galvanized steel. *Mater. Design* 66, 453–458. https://doi.org/10.1016/j.matdes.2014.06.026.

Song, J.L., Lin, S.B., Yang, C.L., Fan, C.L. (2009). Effects of Si additions on intermetallic compound layer of aluminum–steel TIG welding–brazing joint. *J. Alloy. Compd.* 488 (1), 217–222. https://doi.org/10.1016/j.jallcom.2009.08.084.

Squires, L., Lim, Y.C., Miles, M.P., Feng, Z. (2015). Mechanical properties of dissimilar metal joints composed of DP 980 steel and AA 7075-T6. *Sci. Technol. Weld. Joi.* 20 (3), 242–248. https://doi.org/10.1179/1362171815Y.0000000013.

Su, Y., Hua, X., Wu, Y. (2014). Influence of alloy elements on microstructure and mechanical property of aluminum–steel lap joint made by gas metal arc welding. *J. Mater. Process. Tech.* 214 (4), 750–755. https://doi.org/10.1016/j.jmatprotec.2013.11.023.

Torkamany, M.J., Tahamtan, S., Sabbaghzadeh, J. (2010). Dissimilar welding of carbon steel to 5754 aluminum alloy by Nd:YAG pulsed laser. *Mater. Design* 31 (1), 458–465. https://doi.org/10.1016/j.matdes.2009.05.046.

Watanabe, T., Takayama, H., Yanagisawa, A. (2006). Joining of aluminum alloy to steel by friction stir welding. *J. Mater. Process. Tech.* 178 (1–3), 342–349. https://doi.org/10.1016/j.jmatprotec.2006.04.117.

Yang, S., Zhang, J., Lian, J., Lei, Y. (2013). Welding of aluminum alloy to zinc coated steel by cold metal transfer. *Mater. Design* 49, 602–612. https://doi.org/10.1016/j.matdes.2013.01.045.

Yang, J., Li, Y., Zhang, H., Guo, W., Weckman, D., Zhou, N. (2015). Dissimilar Laser Welding/Brazing of 5754 Aluminum Alloy to DP 980 Steel: Mechanical Properties and Interfacial Microstructure. *Metall. Mater. Trans.* A 46 (11), 5149–5157. https://doi.org/10.1007/s11661-015-3079-x.

Zhang, C., Li, G., Gao, M., Yan, J., Zeng, X.Y. (2013). Microstructure and process characterization of laser-cold metal transfer hybrid welding of AA6061 aluminum alloy. *Int. J. Adv. Manuf. Tech.* 68 (5–8), 1253–1260. https://doi.org/10.1007/s00170-013-4916-y.

Zhou, Y., Lin, Q. (2014). Wetting of galvanized steel by Al 4043 alloys in the first cycle of CMT process. *J. Alloy. Compd.* 589, 307–313. https://doi.org/10.1016/j.jallcom.2013.11.177.